

Climate of the Past Discussions is the access reviewed discussion forum of *Climate of the Past*

Proposing a mechanistic understanding of changes in atmospheric CO₂ during the last 740 000 years

P. Köhler and H. Fischer

Alfred Wegener Institute for Polar and Marine Research, P.O. Box 12 01 61, 27515 Bremerhaven, Germany

Received: 15 December 2005 – Accepted: 20 January 2006 – Published: 14 February 2006

Correspondence to: P. Köhler (pkoebler@awi-bremerhaven.de)

© 2006 Author(s). This work is licensed under a Creative Commons License.

1

Abstract

Atmospheric carbon dioxide (CO₂) measured in Antarctic ice cores shows a natural variability of 80 to 100 ppmv during the last four glacial cycles and variations of approximately 60 ppmv in the two cycles between 410 and 650 kyr BP. We here use dust and the isotopic temperature proxy deuterium (δD) from the EPICA Dome C Antarctic ice core covering the last 740 kyr together with other paleo-climatic records to force the ocean/atmosphere/biosphere box model of the global carbon cycle BICYCLE in a forward mode over this time in order to reconstruct the natural variability of pCO_2 . Our simulation results covered by our proposed scenario are based on process understanding gained previously for carbon cycle variations during Termination I. These results match the pCO_2 measured in the Vostok ice core well ($r^2=0.80$) and we predict prior to Termination V significantly smaller amplitudes in pCO_2 variations mainly based on a reduced interglacial ocean circulation and reduced interglacial Southern Ocean sea surface temperature. These predictions for the pre-Vostok period match the new pCO_2 data from the EPICA Dome C ice core for the time period 410 to 650 kyr BP equally well ($r^2=0.79$). This is the first forward modelling approach which covers all major processes acting on the global carbon cycle on glacial/interglacial time scales. The contributions of different processes (terrestrial carbon storage, sea ice, sea level, ocean temperature, ocean circulation, CaCO₃ chemistry, marine biota) are analysed.

20 1 Introduction

Paleo-climatic records derived from ice cores revealed the natural variability in Antarctic temperature (Jouzel et al., 1987), atmospheric dust content (Röthlisberger et al., 2002), and atmospheric CO₂ (Barnola et al., 1987; Fischer et al., 1999; Petit et al., 1999; Monnin et al., 2001; Kawamura et al., 2003; Siegenthaler et al., 2005) over the last glacial cycles. The longest CO₂ record from the Antarctic ice core at Vostok (Petit et al., 1999) went back in time as far as about 410 000 years before present

(410 kyr BP) showing a switch of glacial and interglacials in all those parameters approximately every 100 kyr during the last four glacial cycles with $p\text{CO}_2$ varying between 180–300 ppmv. New measurements of dust and the isotopic temperature proxy δD of the EPICA Dome C ice core covered the last 740 kyr, however, revealed glacial cycles of reduced temperature amplitude (EPICA community members, 2004). These new archives offer the possibility to propose atmospheric CO_2 for the pre-Vostok time span as called for in the EPICA challenge (Wolff et al., 2004). Here, we contribute to this challenge using a box model of the isotopic carbon cycle (Köhler et al., 2005) based on process understanding previously derived for Termination I and show that major features of the Vostok period are reproduced while prior to Termination V our model predicts significantly smaller amplitudes in $p\text{CO}_2$ variations. These pre-Vostok prediction are matched for the time interval 410–650 kyr BP by the new $p\text{CO}_2$ data set measured at EPICA Dome C (Siegenthaler et al., 2005).

The quest of explaining the observed glacial/interglacial variations in atmospheric $p\text{CO}_2$ of about 80–100 ppmv (Petit et al., 1999) was challenging the scientific communities for at least two decades (e.g. Archer et al., 2000; Sigman and Boyle, 2000). Processes which need to be included in solving this quest are the transport of organic and dissolved inorganic carbon (DIC) from the surface to the deep ocean via its physical and biological pumps. Large changes in vertical mixing of the water column (Toggweiler, 1999), changes in the strength of the thermohaline circulation (THC) (Knorr and Lohmann, 2003), variations in sea ice cover in high latitudes limiting gas exchange rates (Stephens and Keeling, 2000; Archer et al., 2003) together with well known temperature and salinity variations (Adkins et al., 2002) of the ocean are processes affecting the carbon cycle via the physical pump. The fertilisation of the marine biological productivity through the aeolian input of iron in areas of high nitrate and low chlorophyll is one theory (Martin, 1990; Ridgwell, 2003) which would reduce atmospheric $p\text{CO}_2$ during glacial times through an enhanced biological export production to the deep ocean. The export of organic carbon itself is closely coupled to the calcium carbonate production of pelagic calcifiers by which CO_2 is released in the surface

3

ocean. Additionally to those processes which distribute DIC, alkalinity and nutrients in the different ocean reservoirs, exchange fluxes of carbon between the terrestrial biosphere and the ocean/atmosphere system (e.g. Joos et al., 2004), riverine input of bicarbonate (Munhoven, 2002), and exchange fluxes of DIC and alkalinity via dissolution and sedimentation between ocean and sediments (Zeebe and Westbroek, 2003) need to be considered to fully understand glacial/interglacial changes in the global carbon cycle.

Previously we put forward a quantitative explanation of observed changes in atmospheric $p\text{CO}_2$ and its carbon isotopes ($\delta^{13}\text{C}$, $\Delta^{14}\text{C}$) using the multi-box model of the global carbon cycle, called BICYCLE, applied to the last glacial termination (Köhler et al., 2005). That study concluded that the main processes impacting on $p\text{CO}_2$ during Termination I were an increase in vertical mixing rates in the Southern Ocean and changes in the DIC and alkalinity inventories through sedimentation and dissolution processes. The time-dependent atmospheric $\delta^{13}\text{C}$ record from the Taylor Dome ice core (Smith et al., 1999) used in that study contains valuable informations, which enabled us to reduce the uncertainties in determining the magnitude and timing of various processes. These results are in that sense robust that the detailed magnitudes of individual processes might vary due to model limitation and data uncertainties, but all their contributions need to be taken into account for explaining the observed variations in the atmospheric carbon records. The still limited knowledge on the size of a marine glacial iron fertilisation effect in the Southern Ocean might be named as largest uncertainty, however, a recent data compilation (Kohfeld et al., 2005) on the role of marine biology on glacial/interglacial CO_2 cycles supports our approach that as a net effect the Southern Ocean marine export production might be a glacial sink for carbon. Assuming that these processes are of general nature, we apply in the following the same model over the time period of the last 740 kyr covered by the EPICA Dome C records to predict $p\text{CO}_2$ variations over the EPICA Dome C era. To this end we forced our model by proxy data from marine and ice core archives.

4

2 Methods

2.1 The BICYCLE model

The Box model of the Isotopic Carbon cYCLE BICYCLE (Köhler et al., 2005) was developed and applied for quantitative interpretation of the atmospheric carbon records ($p\text{CO}_2$, $\delta^{13}\text{C}$, $\Delta^{14}\text{C}$) during Termination I (10–20 kyr BP). The model consists of ten oceanic reservoirs in three different depth layers and distinguishes Atlantic, Indo-Pacific and Southern Ocean (Fig. 1). The strength of the preindustrial ocean circulation as seen in Fig. 1 was parameterised with data from WOCE (Ganachaud and Wunsch, 2000). Marine global export production of 10 PgC yr^{-1} at 100 m water depth (Gnanadesikan et al., 2002) was prescribed for the preindustrial setting, depending on the preformed macro-nutrient concentration of PO_4 in the surface waters. In the equatorial regions all macro-nutrients were utilised for the export production, while in the high latitudes the export production flux was restricted to avoid a global export flux of carbon which exceeds the prescribed 10 PgC yr^{-1} . This led to unutilised nutrient concentrations especially in the Southern Ocean, which can be used for increased marine productivity during times of high aeolian iron input into these regions. The rain ratio of DIC to CaCO_3 in the export production fluxes was kept constant at 10:1 throughout all our simulations. As another boundary condition describing sediment/ocean interactions the lysocline was either kept constant or its variation is prescribed, both leading to fluxes of DIC and alkalinity in the ratio of 1:2 between the deep ocean and the sediments. In doing so we mimic the dissolution or sedimentation of CaCO_3 in the absence of a process-based module of early diagenesis (e.g. Archer et al., 2000). This approach calculates the net changes in the inventories of DIC and alkalinity and therefore implicitly includes changes in the weathering inputs of bicarbonate through rivers. A globally averaged seven-compartment terrestrial biosphere (Köhler and Fischer, 2004) allows photosynthetic production of C_3 and C_4 pathways differing in their isotopic fractionation, and a climate and CO_2 -dependent fixation of carbon on land. A more detailed

5

description of the model is found in Köhler et al. (2005).

2.2 Time-dependent forcing of BICYCLE

We forced BICYCLE forward in time using various paleo-climatic records (Fig. 2). The model applied here used the same parameterisation as for its application on Termination I (Köhler et al., 2005) with the two exceptions that (1) we did not consider a complete shut-down of the North Atlantic Deep Water (NADW) formation during Heinrich events and (2) we selected two scenarios for terrestrial carbon storage which span the range found in the literature. The first change (NADW) is based on productivity results (Sachs and Anderson, 2005) and sea level fluctuations (Siddall et al., 2003) that indicate that Heinrich events during MIS 2 and 3 may have caused different perturbations to the ocean circulation. It is therefore not possible to generalise changes in NADW formation throughout the EPICA Dome C period. Nevertheless, we discuss the potential impact of Heinrich events in Sect. 3.2. The second change was performed to highlight the error propagation of the still existing uncertainties in the glacial/interglacial rise in carbon stored on land onto atmospheric $p\text{CO}_2$.

Because various records that were used to force our model had a rather coarse resolution we have chosen to smooth all forcing records and all simulation results and concentrate on low frequency changes in the carbon cycle.

The relevant forcing functions were adapted as follows:

Ocean temperature: Reconstructed summer SST at ODP980 (McManus et al., 1999; Wright and Flower, 2002) (using modern analogue techniques in the times before 500 kyr (Wright and Flower, 2002)) was used as proxy for SST changes in the North Atlantic (north of 50°N) scaled to a glacial/interglacial amplitude during Termination I of 4 K (Fig. 2b). SSTs of equatorial surface oceans were estimated from planktic $\delta^{18}\text{O}$ measured in ODP677 in the equatorial Pacific (Shackleton et al., 1990) scaled to a glacial/interglacial amplitude during Termination I of 3.75 K (Visser et al., 2003) which was already used previously (Fig. 2d). Southern Ocean (south of 40°S) SST with a glacial/interglacial amplitude during Termination I of 4 K was estimated from δD of the

6

EPICA Dome C ice core (EPICA community members, 2004) (Fig. 2h). Here, EPICA Dome C δD was corrected for the effect of sea level changes (Jouzel et al., 2003) using a normalised record of sea level change from Bintanja et al. (2005).

Sea ice: Varying sea ice coverage will influence the gas exchange rates between the atmosphere and the surface ocean. We coupled time-dependent changes in the sea ice area in the North Atlantic and the Southern Ocean on the assumed temperature changes in the respective surface ocean boxes. Present day annual mean sea ice area was set to $10 \times 10^{12} \text{ m}^2$ in each hemisphere (Cavalieri et al., 1997). During the LGM the annual average area covered by sea ice increased to $14 \times 10^{12} \text{ m}^2$ in the North and $22 \times 10^{12} \text{ m}^2$ in the South based on various studies (Crosta et al., 1998a,b; Sarnthein et al., 2003; Gersonde et al., 2005). In addition to changing surface box area due to sea level change this results in a relative areal coverage of 50 and 85% in the North Atlantic box and 13 and 30% in the Southern Ocean box during preindustrial times and the LGM, respectively.

Sea level: We used the results of Bintanja et al. (2005) on changes in sea level (Fig. 2f). This modelling study is based on a benthic $\delta^{18}\text{O}$ stack from 57 globally distributed sediment core covering more than the last 5 million years (Lisiecki and Raymo, 2005).

Ocean circulation: There are data- and model-based evidences for a reduced ocean overturning in the Atlantic and the Southern Ocean, while the glacial circulation in the Pacific Ocean seemed to have been similar to today's (Meissner et al., 2003; Hodell et al., 2003; Knorr and Lohmann, 2003; Broecker et al., 2004; McManus et al., 2004; Watson and Garabato, 2006). It was shown (Flower et al., 2000) that the depth gradient in $\delta^{13}\text{C}$ which is an indicator for the strength in NADW formation is highly correlated with benthic $\delta^{18}\text{O}$. To rely on as few different cores as possible and thus to minimise timing uncertainties we therefore used benthic $\delta^{18}\text{O}$ in ODP980 (McManus et al., 1999; Flower et al., 2000) as a proxy for the strength in NADW formation bearing in mind that this might introduce a possible phase shift of the contribution of changes in NADW formation on $p\text{CO}_2$ (Fig. 2c). We defined $\delta^{18}\text{O}_{\text{NADW}} = 2.8\text{‰}$ as a threshold for changes

7

in the Atlantic thermohaline circulation. The strength of NADW formation of 16 Sv ($1 \text{ Sv} = 10^6 \text{ m}^3 \text{ s}^{-1}$) during interglacial periods ($\delta^{18}\text{O} < 2.8\text{‰}$) was based on the World Ocean Circulation Experiment WOCE (Ganachaud and Wunsch, 2000), the strength of 10 Sv during glacial times ($\delta^{18}\text{O} \geq 2.8\text{‰}$) on various modelling studies (e.g. Meissner et al., 2003). The net vertical water mass exchange fluxes in the Southern Ocean was coupled linearly to Southern Ocean temperature changes with 29 Sv during preindustrial SST and 9 Sv during the LGM. Southern Ocean deep water ventilation would also be reduced due to the glacial reduction of NADW formation by 6 Sv and its subsequent fluxes. An instantaneously switching from glacial to interglacial mixing rates in the Southern Ocean as used previously (Köhler et al., 2005) was not necessary here due to the low resolution of all forcing records. Changing ocean circulation fluxes are depicted in bold in Fig. 1.

Marine biota: Due to the prescribed export production fluxes in our reference scenario there exist unutilised macro-nutrients in the Southern Ocean surface waters. In these high nutrient low chlorophyll areas an increased export production in times of high aeolian iron input might occur as described in the iron fertilisation hypothesis (Martin, 1990; Ridgwell, 2003). The atmospheric dust content of the EPICA Dome C ice core (EPICA community members, 2004) was used as proxy for aeolian input of iron into the Southern Ocean which might enhance marine biological productivity there if allowed by macro-nutrient availability (Fig. 2i). We keep a similar threshold ($\text{dust}_{\text{Fe}} > 310 \text{ ppbv}$) as deduced for Termination I (Köhler et al., 2005) above which iron fertilisation might occur. Increased export production was then coupled linearly to increased dust concentrations.

Terrestrial biosphere: The changing terrestrial carbon storage depends on the internally calculated CO_2 concentration (CO_2 fertilisation) and average global temperature, the latter calculated as 3:1 mixture of northern and southern hemispheric temperature with glacial/interglacial amplitudes of 8 and 4 K, respectively (Köhler and Fischer, 2004; Köhler et al., 2005). Temperature changes were forced by simulation results from Bintanja et al. (2005) for the North, who calculated the average northern (40–

8

80° N) hemispheric temperature changes as a function of sea level variations and thus northern land ice sheet distribution based on the stacked benthic $\delta^{18}\text{O}$ record of Lisiecki and Raymo (2005) (Fig. 2e), and by EPICA Dome C δD for the South (Fig. 2h). Glacial/interglacial fluctuations in terrestrial carbon is with about 1000 PgC at the upper range predicted by various modelling and data based studies (see review in Köhler and Fischer, 2004). Alternative smaller glacial/interglacial changes in terrestrial carbon storage are investigated in a sensitivity study.

CaCO₃ chemistry: All changes in the carbon cycle alter the concentration of the CO₃²⁻ ion in the deep ocean. As a consequence the saturation horizon of CaCO₃ varies, which then induces changes in either the dissolution or sedimentation rates, a process known as CaCO₃ compensation (Broecker and Peng, 1987). In the absence of a process-based model of early diagenesis, which would cover these processes, we here calculated sediment/deep ocean fluxes of calcium carbonate (changing deep ocean DIC and alkalinity in a ratio of 1:2) by the application of an additional boundary condition. We forced our model to reconstruct observed variations in the temporal changes of the lysocline. The lysocline is the oceanic depth below which sedimentary calcite dissolves and is approximated in our model with the saturation depth of calcite, which is calculated as a function of depth (pressure) in vertical steps of 200 m and interpolated in-between. The variations in the depth of the Pacific lysocline were derived from CaCO₃ preservation of 17 cores located between 3903 and 4949 m water depth (Farrell and Prell, 1989) (Fig. 2g). The lysocline in the Atlantic and the Southern Ocean was in a first step assumed to be constant, while later on variations in these two ocean basins on our results were investigated. This approach covers changes in the net fluxes of DIC and alkalinity, and thus implicitly includes riverine inputs of bicarbonate through weathering (Munhoven, 2002).

3 Results

3.1 Reconstruction of low frequency changes in atmospheric $p\text{CO}_2$

The simulation results of atmospheric $p\text{CO}_2$ in our standard scenario (Fig. 2j) show high correlations with both the Vostok ($r^2=0.80$ in the time window 0–410 kyr BP) and the EPICA Dome C ($r^2=0.79$; 410–650 kyr BP) $p\text{CO}_2$ records (Petit et al., 1999; Siegenthaler et al., 2005). Our model reproduces the natural variability in $p\text{CO}_2$ ranging from 180 ppmv during glacial maxima to 260 ppmv in the interglacial periods between Marine Isotope Stage (MIS) 13 and 17 and 280 ppmv during the last four interglacials. The agreement in terms of timing and amplitude of changes is especially remarkable during terminations, but fails to reproduce some features of the data records:

(A) The timing in the simulation of $p\text{CO}_2$ reductions during some glaciations is incorrect. This might be largely caused by an earlier decrease in the Antarctic ice core temperature proxies δD than in the Southern Ocean sea surface temperature (SST). From the deuterium excess record in the ice (Vimeux et al., 2002) it is known that the temperature change in the source regions of the precipitated moisture lags Antarctic temperature during glaciations.

(B) We fail to reproduce the $p\text{CO}_2$ maxima of 300 ppmv in MIS 9. As our model is driven by various paleo-climatic archives plotted on their individual age scales and of low temporal resolution (~ 1 kyr) especially the reproduction of peak values in $p\text{CO}_2$ depends on the temporal matching of these driving records. Therefore, our results here have to be understood as an estimate of low frequency fluctuations in $p\text{CO}_2$. Furthermore, coral reef growth which increases $p\text{CO}_2$ during sea level high stands (Vecsei and Berger, 2004) is not considered so far leaving space for interpretation during interglacial times in which sea level rose above 70 m below present and the main shelves were flooded.

(C) A major excursion between simulation and data at 150–180 kyr BP occurs at times of high fluctuations in the atmospheric dust content crossing several times the threshold which indicates the start in iron fertilisation in the Southern Ocean (Fig. 2i). This

simple parametrisation of iron fertilisation is responsible for the third mismatch indicating the limitations of our approach here. The consequences of this simple approach are analysed in detail in our sensitivity study in the next subsection.

(D) Finally, our simulations do not reconstruct fast fluctuations in $p\text{CO}_2$ as seen in the EPICA Dome C $p\text{CO}_2$ record in MIS 15 around 600 kyr BP. At least 20–30 ppmv, about half of the amplitudes seen in the $p\text{CO}_2$ record, can be explained, if a more accurate and higher resolved record of EPICA Dome C δD (J. Jouzel et al., unpublished data) for the earlier parts of the ice core record is taken for forcing the model. The uncertainty in the age model in this time period (Brook, 2005) might also be responsible for parts of the offset.

In the pre-Vostok period covered by EPICA Dome C (for which $p\text{CO}_2$ data were not available during the call of the EPICA challenge) both the regularity and the amplitude in atmospheric $p\text{CO}_2$ as proposed with our model differ from those of the Vostok period (Fig. 2j). Peak values during interglacial periods in MIS 13, 15, and 17 reach 250–260 ppmv, with 70 to 120 kyr elapsing in-between. Atmospheric $p\text{CO}_2$ drops during glacials in MIS 12, 14, and 16 to 180–200 ppmv.

Our simulations suggest that the smallest glacial/interglacial rise in $p\text{CO}_2$ of 50 ppmv occurred from MIS 14 to MIS 13 across Termination VI, about half of the amplitudes which are simulated across the Terminations I to V; the impact of Termination VII on $p\text{CO}_2$ seemed to have been of average magnitude (Fig. 3). The tendency of cooler and longer interglacials as seen in the EPICA Dome C δD data (EPICA community members, 2004) is also mirrored by our proposed $p\text{CO}_2$ record. According to our model the $p\text{CO}_2$ concentration in the pre-Vostok period remained longer at relatively high levels, but with smaller glacial/interglacial amplitudes compared to the Vostok period. Again, the low frequency variations as seen in the new EPICA Dome C $p\text{CO}_2$ record are matched by our standard scenario very well.

In two sensitivity analyses the importance of individual processes were investigated by (a) excluding one process from time-dependent forcings (Fig. 4) and (b) forcing only one process at a time (Fig. 5). From these analyses we estimate the contributions

11

of individual processes to the rise in $p\text{CO}_2$ during the last eight terminations (Fig. 6) keeping in mind the limited validity of the absolute values due to the high non-linearities of the simulated system. The contributions (estimated by excluding one process from time-dependent forcings) in decreasing order to the rise in $p\text{CO}_2$ are given by changes in exchange fluxes between ocean and sediment (on average 38 ppmv during Termination I to V and 21 ppmv earlier), Southern Ocean vertical mixing (38/20 ppmv), iron fertilisation in the Southern Ocean (22/14 ppmv), ocean temperature (21/8 ppmv), and NADW formation (9/–1 ppmv). Changes in sea level (–13/–6 ppmv), gas exchange caused by sea ice cover (–9/–8 ppmv), and terrestrial carbon storage (–25/–14 ppmv) were processes enlarging the observed $p\text{CO}_2$ rise by up to 50 ppmv during terminations. While most processes are reduced in their magnitude prior to Termination V, the absolute contribution of iron fertilisation changes only slightly. Thus, the relative importance of biogeochemical processes including CaCO_3 chemistry is enhanced from 45% to 60% during earlier terminations. The contribution of physical processes (SST, sea level, sea ice) to the $p\text{CO}_2$ rise during terminations stays always below 20%, while ocean circulation contributed on average 50% during the Vostok period (including Termination V), but only 30–40% during Termination VII (Fig. 6).

In the single process analysis following the one-at-a-time approach (Fig. 5, Fig. 6) one has to keep in mind two limitations regarding the contributions from the terrestrial carbon stocks and from the CaCO_3 chemistry. (1) Carbon storage on land is itself a function of atmospheric $p\text{CO}_2$ through the CO_2 fertilisation of photosynthesis. Therefore, in a single process analysis variations in terrestrial carbon storage depict only those changes caused by the change in global temperature, but not by the CO_2 concentration. The $p\text{CO}_2$ variations in Fig. 5 TB are based on a glacial/interglacial variation in terrestrial carbon storage of about 130 PgC, and not of more than 1000 PgC as simulated in our standard scenario. (2) The estimation of CaCO_3 chemistry processes on the changes in $p\text{CO}_2$ in the one-at-a-time approach (Fig. 5 CA, Fig. 6) finds only a contribution of several ppmv (<5 ppmv), which derives from of the change in the depth of the lysocline. In simulations in which all other processes acting on the carbon cycle are also

12

operating the CaCO_3 chemistry responses to deep ocean CO_3^{2-} concentration and the impact on atmospheric $p\text{CO}_2$ is one order of magnitude larger.

As mentioned by Brook (2005) the EDC2 age model (Schwander et al., 2001) which has been used for all EPICA Dome C records here, might need a revision in the times covering MIS 13 to 15. Our simulations point in the same direction: In general, sea level maxima occur during warm interglacial periods, while sea level minima fall together with minimum temperatures. This is the case for the sea level reconstruction based on benthic $\delta^{18}\text{O}$ data (Bintanja et al., 2005) and δD from EPICA Dome C for the last 450 kyr (Fig. 2). During MIS 13 to 15 these two records are out of phase, which is probably caused by chronological uncertainties in the EPICA Dome C records caused by anomalies in ice flow. An updated chronology correcting for these mismatches is currently developed (F. Parrenin et al., unpublished manuscript). The implication of this chronological artefact in the Dome C data sets is, that our reconstruction of $p\text{CO}_2$ across Termination VI is biased. For example, the contribution from sea level rise during Termination VI is positive, opposing its signal during all other glacial/interglacial transitions (Fig. 6). This leads also to a very small estimate of the $p\text{CO}_2$ during Termination VI in the sum of all processes estimated from the sensitivity analysis which excludes one process from time-dependent forcings (Fig. 3).

Termination VIII has also to be taken with caution as EPICA Dome C δD data prior to 740 kyr BP (J. Jouzel et al., unpublished data) reveal that minimum temperatures and thus full glacial conditions in MIS 18 are reached in even older times.

3.2 Model sensitivity

Our approach proposes a decline of $p\text{CO}_2$ by ~ 10 ppmv during terminations contributed by changes in the gas exchange rate through the shrinking of sea ice coverage. This would contradict a previous modelling study (Stephens and Keeling, 2000) which concluded that a nearly full sea ice coverage of the Southern Ocean south of 55°S would reduce $p\text{CO}_2$ by 67 ppmv. Although the reliability of this previous study was

13

questioned because of the proposed very high sea ice coverage (Morales-Maqueda and Rahmstorf, 2001) the question remains why our model responses in the opposite direction. It was already shown (Archer et al., 2003) that a model response to a fully Southern Ocean sea ice coverage is highly model depending. In our study the rise in $p\text{CO}_2$ during deglaciations is caused by larger gas exchange rate in the North Atlantic Ocean which itself is caused by the decrease in the northern sea ice cover. As the modern North Atlantic is a sink for CO_2 while the Southern Ocean is a source, reducing gas exchange during glacials in the North is increasing the glacial atmospheric $p\text{CO}_2$. The net effect of sea ice coverage in the Southern Ocean is negligible and reaches the magnitude of the North only when the Southern Ocean surface box is nearly fully covered by sea ice (Fig. 7). However, our data based assumption proposes only an average annual glacial sea ice coverage of 30% in our Southern Ocean surface box. We therefore have to acknowledge that this effect is model dependent. Furthermore, in our single process analysis we consider only the effect of sea ice on gas exchange rates, while in the previous studies the overall effect of sea ice on both gas exchange and ocean circulation schemes was analysed. Measurements on gas exchange through sea ice of different temperature come to the conclusions, that gas exchange is not totally prevented by a complete sea ice cover, (Gosink et al., 1976; Semiletov et al., 2004). Therefore, we believe that the impact of sea ice cover on the global carbon cycle is not yet fully understood.

In our reference scenario we have chosen to keep NADW formation unchanged during Heinrich events as there are evidences from productivity (Sachs and Anderson, 2005) and sea level (Siddall et al., 2003) reconstructions, that the impact may differ. Here, we estimate the maximum impact through a complete shut-down of NADW formation during Heinrich events identified by ice rafted debris (IRD) in the North Atlantic sediment record ODP980 measured on the same core than two other paleo records used already in our study (North Atlantic SST and benthic $\delta^{18}\text{O}$) (McManus et al., 1999; Wright and Flower, 2002). IRD in percentage of sediment grains larger than $150\ \mu\text{m}$ (relative IRD) is a proxy for the occurrence of Heinrich events (Heinrich, 1988).

14

We used the relative strength $IRD_H=10\%$ as threshold indicating large iceberg and thus freshwater discharges occurring in the North Atlantic which result in a complete shut-down of the NADW formation during glacial times in our model. This threshold was derived from the analysis of IRD and known Heinrich events during the last glacial cycle (Heinrich, 1988). During two time intervals relative IRD data were missing in ODP980 (740–700 and 543–500 kyr BP). The absolute IRD record (lithics/g) spanned our whole simulation period (Wright and Flower, 2002) and showed no major excursions in the incomplete periods of the relative IRD record apart from one large peak during the period 740–700 kyr BP. However, this absolute record is unsuitable for the predictions of Heinrich events as known events occurring during the last glacial cycle (Heinrich, 1988) would have been overestimated. IRD in a second core approximately 1000 km apart (ODP984) shows similar features during 500–740 kyr BP (Wright and Flower, 2002) suggesting an at least regional distribution of the IRD signals measured in ODP980 and the changes in freshwater discharge indicated by them.

A shut-down of the NADW formation occurring during the Heinrich events, which were identified by the relative IRD record, reduces atmospheric pCO_2 during glacial climate conditions by about 10 ppmv (Fig. 4). Only a Heinrich event around 550 kyr BP happening during intermediate climate conditions would lead to a sharp drop in pCO_2 by more than 30 ppmv. The selection criteria for Heinrich events ($IRD_H=10\%$) was varied in a sensitivity study (Fig. 8b), and showed rather unchanged response of pCO_2 for a threshold increase by a factor of two, and an extension of Heinrich events if IRD_H was lowered.

The impacts of the other two thresholds on modelled processes ($\delta^{18}O_{NADW}$ in ODP980 as regulator for the strength of NADW formation; $dust_{Fe}$ in EPICA Dome C as indicator for iron fertilisation in the Southern Ocean) were also tested (Fig. 8). The strength in the NADW formation during interglacial times depends to a certain extent on the chosen threshold which indicates a switch from glacial to interglacial circulation patterns in the Atlantic Ocean (Fig. 8a). The NADW formation strength during warm periods around 200 kyr BP and in the pre-Vostok time is only switching into its inter-

15

glacial mode (16 Sv), when the threshold parameter is increased leading to a rise in pCO_2 by about 10 ppmv. The impact of Southern Ocean iron fertilisation on pCO_2 (Fig. 8c) varies only if its dependency on EPICA Dome C dust content is altered by one order of magnitude and during the high dust fluctuations around 150–180 kyr BP. We therefore consider our results during 150–180 kyr BP to be influenced by our approach of simulating iron fertilisation and as fairly robust otherwise.

It was argued recently that based on the knowledge gained from experiments only 0.5 to 15% of the the glacial/interglacial rise in pCO_2 can be caused by iron fertilisation of the marine biota (de Baar et al., 2005). However, their estimate was based on the assumption that the glacial aeolian iron input into the Antarctic region was 11-fold its modern flux, while data from EPICA Dome C find increases in iron fluxes (Wolff et al., 2006) and non-sea salt dust fluxes (Röthlisberger et al., 2002) from interglacial to glacial periods by a factor of 25. We therefore believe that the implications of iron fertilisation experiments for questions of glacial/interglacial pCO_2 rise do not limit the impact of iron onto the global carbon cycle in the way as proposed by de Baar et al. (2005). With this different interpretation our simulation results, which propose a contribution of this process of approximately 25%, are still within the range covered by iron fertilisation experiments (1–34%).

It is known that the depth variations of the lysocline in the Atlantic and the Southern Ocean were opposing those trends seen in the Pacific Ocean (Curry and Lohmann, 1986; Crowley, 1983; Howard and Prell, 1994). Due to missing data sets of lysocline variations in these two ocean basins over the whole simulation period the lysocline in the Atlantic and the Southern Ocean was kept constant in our standard simulation. We tested the importance of this simplification by further sensitivity scenarios, in which either all lysoclines were kept constant, or all were varied similar to the Pacific data set of Farrell and Prell (1989) (Fig. 9). Atmospheric pCO_2 variations are less than 5 ppmv different in these additional simulations than in our standard scenario. This implies, that the calculation of exchange fluxes of DIC and alkalinity itself to counterbalance changes in deep ocean CO_3^{2-} concentration is very important, but the precise knowledge of the

16

lyscoline is of minor relevance in the model.

To cover the estimated range in the glacial/interglacial rise in terrestrial carbon storage of 300–1100 PgC (Köhler and Fischer, 2004) an alternative scenario S_TB- with reduced variability of the terrestrial biosphere was investigated. Terrestrial carbon storage varies during Termination I by about 500 PgC in S_TB- and 1100 PgC in the standard scenario S (Fig. 10b). The change in the amplitude in terrestrial carbon storage leads also to different CaCO₃ fluxes between sediment and deep ocean and thus to different fluctuations in the overall carbon budget. While total carbon of the simulated ocean-atmosphere-biosphere system is 1700 PgC larger in the LGM if compared with preindustrial times in scenario S, this glacial carbon rise is reduced to 1200 PgC in scenario S_TB- (Fig. 10c). This additional carbon during glacial conditions enters the simulated system from the sediments. As overall effect glacial atmospheric $p\text{CO}_2$ is about 15 ppmv lower in scenario S_TB- than in S (Fig. 10a). Our scenarios cover a large part of the range of changes in terrestrial carbon storage proposed by different studies. The overall impact of different terrestrial carbon storage on $p\text{CO}_2$ is small.

Finally, we investigated the sensitivity of our model to the amplitudes in these eight different processes contributing to the glacial/interglacial $p\text{CO}_2$ rise. We therefore varied their glacial/interglacial amplitudes by up to $\pm 50\%$ from their standards and compared the relative impacts on $p\text{CO}_2$ for Termination I (Fig. 11). The sensitivity of the modelled $p\text{CO}_2$ to changes in the amplitude of one process is rather linear. Varying amplitudes by less than 20% would result in less than ~ 5 ppmv deviation in $p\text{CO}_2$. We therefore evaluate our model as rather robust to the detailed knowledge of individual processes.

4 Discussion

Our study proposes a mechanistic understanding of the global carbon cycle which enables us to reconstruct low frequency changes in the natural carbon cycle on glacial timescales. The simulation results match atmospheric $p\text{CO}_2$ during the last 650 kyr

17

rather well ($r^2 \sim 0.8$) and we propose $p\text{CO}_2$ variations back to 740 kyr BP to be confirmed by future measurements of $p\text{CO}_2$ enclosed in air bubbles in Antarctic ice cores. The novelty of our approach is the fact that the process understanding how the global carbon cycle including its isotopes is operating during Termination I seems to be sufficient to explain atmospheric $p\text{CO}_2$ not only during the regular variations observed in the Vostok ice core but also to predict correctly smaller glacial/interglacial amplitudes prior to Termination V. The application of our model to this long timescales is in a way a confirmation that our assumptions made for and our understanding gained from a detailed reconstruction during Termination I (Köhler et al., 2005) are not restricted to this very narrow time window, but are of general nature.

Our results are further supported by reconstructed pH in the equatorial Atlantic surface waters, which are based on $\delta^{11}\text{B}$ measurements from planktic foraminifers (Hönisch and Hemming, 2005). As we calculate the whole carbonate system in our model, we are able to compare our simulated pH variations in the surface water box of the equatorial Atlantic with these measurements (Fig. 12). Although the data set is very sparse (16 data points over two glacial cycles) our model predicts a similar glacial/interglacial amplitude of 0.15 in this area. Minima during interglacial periods are smaller in the data than in the model. The difference between simulation and data during MIS 9 (~ 330 kyr BP) are very probably caused by our simulation results, as we are also unable to reconstruct $p\text{CO}_2$ very accurately here. For the other differences it is so far not clear if they are caused by local effects recorded in $\delta^{11}\text{B}$ or model uncertainties. The reorganisation of the carbon cycle during interglacial periods such as the Holocene, in which $p\text{CO}_2$ varied by about 20 ppmv (Indermühle et al., 1999) is not within the scope of this work. Various alternative scenarios based on data analysis and more complex models were already proposed for the interpretation of the Holocene $p\text{CO}_2$ record (e.g. Broecker et al., 2001; Brovkin et al., 2002; Ridgwell et al., 2003; Ruddiman, 2003; Joos et al., 2004; Wang et al., 2005). Further details on carbon cycle variations during the last glacial cycle, for which more and more accurate $p\text{CO}_2$

data exist, are found in Köhler et al. (2006)¹.

To our knowledge, there exist so far two transient modelling approaches which try to explain atmospheric $p\text{CO}_2$ during the late Pleistocene both using conceptual models (Gildor et al., 2002; Paillard and Parrenin, 2004) and concentrate on changes in ocean physics. These two approaches differ widely, one (Gildor et al., 2002) being purely theoretically and trying to explain the typical amplitude and seesaw shape of $p\text{CO}_2$ observed in Vostok, while the other (Paillard and Parrenin, 2004) is forced by insolation over the last 1000 kyr. However, both pinpoint reduced glacial vertical mixing in the Southern Ocean as one mechanism which contributes significantly to the glacial/interglacial rise in $p\text{CO}_2$. While we here support the importance of changes in Southern Ocean vertical mixing, we also want to point out that especially those processes which modify the overall budgets of DIC and alkalinity in the ocean need some considerations (Archer et al., 2000) and a restricted view onto the ocean/atmosphere carbonate system only is of limited validity for a complete understanding of the observed changes in the carbon cycle as recorded in the ice cores.

One result of the EPICA challenge was that all approaches using existing Antarctic temperature proxies and simple regression functions were able to predict $p\text{CO}_2$ with high accuracy (Wolff et al., 2005). Can we understand this coupling of atmospheric $p\text{CO}_2$ and Antarctic/Southern Ocean temperature from our process-based modelling approach? SST of the Southern Ocean itself is according to our model responsible for half of the rise in $p\text{CO}_2$ caused by ocean temperature, which would be ~ 15 ppmv during Termination I. Changes in sea ice cover and Southern Ocean vertical mixing are in BICYCLE functions of Southern Ocean SST, causing 0 ppmv and 35 ppmv, respectively. As discussed earlier the contribution of Southern Ocean sea ice cover is model dependent and should therefore be taken with caution. Furthermore, CaCO_3 compen-

¹ Köhler, P., Muscheler, R., and Fischer, H.: A model-based interpretation of low frequency changes in the carbon cycle during the last 120 kyr and its implications for the reconstruction of atmospheric $\Delta^{14}\text{C}$ and the geomagnetic field strength, *Geochemistry, Geophysics, Geosystems*, in review, 2006.

sation is a responding process on changes in deep ocean CO_3^{2-} concentration. Let us assume that its contribution of 40 ppmv to the simulated rise of 80 ppmv might be linearly coupled to perturbations in the carbon cycle caused by other processes. Taken all the mentioned processes together (direct effect of Southern Ocean SST: 15 ppmv; indirect effects: 35 ppmv; CaCO_3 amplifier: $50/80 \times 40$ ppmv = 25 ppmv) we are able to explain already a rise in $p\text{CO}_2$ of 75 ppmv during Termination I only by direct and indirect effects of Southern Ocean temperature changes. However, this is an incomplete solution, because other changes in the carbon cycle are known to have happened, such as changing concentration of DIC due to sea level variations or changing carbon storage on land which would both operate in the opposite direction.

Although this box model study provides only a rough estimate of low frequency changes in $p\text{CO}_2$ during the past 740 kyr, it nevertheless is the first modelling approach which includes all major processes, whose contributions to the variations in atmospheric $p\text{CO}_2$ need to be considered. The other seven entries to the EPICA challenge (Wolff et al., 2005) were able to reproduce Vostok $p\text{CO}_2$ data with similar accuracy. However, they were either based on a conceptual modelling approach (Paillard and Parrenin, 2004) or on different correlation functions of the two EPICA Dome C records (dust, δD) and others paleo-climatic archives. Thus, they all tested different hypotheses, but were per se unable to gain a process understanding of the glacial/interglacial variability of the carbon cycle as proposed here. It is furthermore remarkable that our approach does not only reconstruct the rather regular variations in $p\text{CO}_2$ as seen in Vostok but is also able to predict correctly the smaller interglacial $p\text{CO}_2$ values as indeed measured in the EPICA Dome C ice core (Siegenthaler et al., 2005).

Acknowledgements. This study was performed within the RESPIC project, funded through the German Climate Research Programme DEKLIM (BMBF). R. Bintanja, B. Hönisch, J. Jouzel, V. Masson-Delmotte, J. McManus and U. Siegenthaler kindly provided data sets. We like to thank the EPICA challenge team for the inspiring scientific quest. This work is a contribution to the European Project for Ice Coring in Antarctica (EPICA), a joint European Science

Foundation/European Commission scientific programme, funded by the EU (EPICA-MIS) and by national contributions from Belgium, Denmark, France, Germany, Italy, the Netherlands, Norway, Sweden, Switzerland and the United Kingdom. This is EPICA publication no. 145.

References

- 5 Adkins, J. F., McIntyre, K., and Schrag, D. P.: The salinity, temperature, and $\delta^{18}\text{O}$ of the glacial deep ocean, *Science*, 298, 1769–1773, 2002. [3](#)
- Archer, D., Winguth, A., Lea, D., and Mahowald, N.: What caused the glacial/interglacial atmospheric $p\text{CO}_2$ cycles?, *Rev. Geophys.*, 38, 159–189, 2000. [3](#), [5](#), [19](#)
- 10 Archer, D. E., Martin, P. A., Milovich, J., Brovkin, V., Plattner, G.-K., and Ashendel, C.: Model sensitivity in the effect of Antarctic sea ice and stratification on atmospheric $p\text{CO}_2$, *Paleoceanography*, 18, 1012, doi:10.1029/2002PA000760, 2003. [3](#), [14](#)
- Barnola, J. M., Raynaud, D., Korotkevich, Y. S., and Lorius, C.: Vostok ice core provides 160,000-year record of atmospheric CO_2 , *Nature*, 329, 408–414, 1987. [2](#)
- 15 Bintanja, R., van der Wal, R., and Oerlemans, J.: Modelled atmospheric temperatures and global sea levels over the past million years, *Nature*, 437, 125–128, doi:10.1038/nature03975, 2005. [7](#), [8](#), [13](#), [30](#)
- Broecker, W., Barker, S., Clark, E., Hajdas, I., Bonani, G., and Stott, L.: Ventilation of the glacial deep Pacific Ocean, *Science*, 306, 1169–1172, 2004. [7](#)
- Broecker, W. S. and Peng, T.-H.: The role of CaCO_3 compensation in the glacial to interglacial atmospheric CO_2 change, *Global Biogeochem. Cycles*, 1, 15–29, 1987. [9](#)
- 20 Broecker, W. S., Lynch-Stieglitz, J., Clark, E., Hajdas, I., and Bonani, G.: What caused the atmosphere's CO_2 content to rise during the last 8000 years?, *Geochem. Geophys. Geosyst.*, 2, doi:2001GC000177, 2001. [18](#)
- Brook, E. J.: Tiny bubbles tell all, *Science*, 310, 1285–1287; doi:10.1126/science.11211535, 2005. [11](#), [13](#)
- 25 Brovkin, V., Bendtsen, J., Claussen, M., Ganopolski, A., Kubatzki, C., Petoukhov, V., and Andreev, A.: Carbon cycle, vegetation, and climate dynamics in the Holocene: Experiments with the CLIMBER-2 model, *Global Biogeochem. Cycles*, 16, 1139, doi:10.1029/2001GB001662, 2002. [18](#)

- Cavalieri, D. J., Gloersen, P., Parkinson, C. L., Comiso, J. C., and Zwally, H. J.: Observed hemispheric asymmetry in global sea ice changes, *Science*, 278, 1104–1106, 1997. [7](#)
- Crosta, X., Pichon, J.-J., and Burckle, L. H.: Application of modern analog technique to marine Antarctic diatoms: Reconstruction of maximum sea-ice extent at the Last Glacial Maximum, *Paleoceanography*, 13, 284–297, 1998a. [7](#)
- 5 Crosta, X., Pichon, J.-J., and Burckle, L. H.: Rearaisal of Antarctic seasonal sea-ice extent at the Last Glacial Maximum, *Geophys. Res. Lett.*, 14, 2703–2706, 1998b. [7](#)
- Crowley, T. J.: Calcium-carbonate preservation patterns in the central North Atlantic during the last 150 000 years, *Marine Geology*, 51, 1–14, 1983. [16](#)
- 10 Curry, W. B. and Lohmann, G. P.: Late Quaternary carbonate sedimentation at the Sierra Leone rise (eastern equatorial Atlantic Ocean), *Marine Geology*, 70, 223–250, 1986. [16](#)
- de Baar, H. J. W., Boyd, P. W., Coale, K. H., Landry, M. R., Tsuda, A., Assmy, P., Bakker, D. C. E., Bozec, Y., Barber, R. T., Brzezinski, M. A., Buesseler, K. O., Boyé, M., Croot, P. L., Gervais, F., Gorbunov, M. Y., Harrison, P. J., Hiscock, W. T., Laan, P., Lancelot, C., Law, C. S., 15 Lvasseur, M., Marchetti, A., Millero, F. J., Nishioka, J., Nojiri, Y., van Oijen, T., Riebesell, U., Rijkenberg, M. J. A., Saito, H., Takeda, S., Timmermans, K. R., Veldhuis, M. J. W., Waite, A. M., and Wong, C.-S.: Synthesis of iron fertilization experiments: From the Iron Age in the Age of Enlightenment, *J. Geophys. Res.*, 110, C09S16, doi:10.1029/2004JC002601, 2005. [16](#)
- 20 EPICA community members: Eight glacial cycles from an Antarctic ice core, *Nature*, 429, 623–628, 2004. [3](#), [7](#), [8](#), [11](#), [30](#)
- Farrell, J. W. and Prell, W. L.: Climate change and CaCO_3 preservation: An 800 000 year bathymetric reconstruction from the central equatorial Pacific Ocean, *Paleoceanography*, 4, 447–466, 1989. [9](#), [16](#), [30](#)
- 25 Fischer, H., Wahlen, M., Smith, J., Mastroianni, D., and Deck, B.: Ice core records of atmospheric CO_2 around the last three glacial terminations, *Science*, 283, 1712–1714, 1999. [2](#)
- Flower, B. P., Oppo, D. W., McManus, J. F., Venz, K. A., Hodell, D. A., and Cullen, J. L.: North Atlantic intermediate to deep water circulation and chemical stratification during the past 1 Myr, *Paleoceanography*, 15, 388–403, 2000. [7](#), [30](#)
- 30 Ganachaud, A. and Wunsch, C.: Improved estimates of global ocean circulation, heat transport and mixing from hydrographic data, *Nature*, 408, 453–457, 2000. [5](#), [8](#), [28](#)
- Gersonde, R., Crosta, X., Abelmann, A., and Armand, L.: Sea-surface temperature and sea ice distribution of the Southern Ocean at the EPILOG Last Glacial Maximum – a circum-

- Antarctic view based on siliceous microfossil records, *Quat. Sci. Rev.*, 24, 869–896, 2005. [7](#)
- Gildor, H., Tziperman, E., and Toggweiler, J. R.: Sea ice switch mechanism and glacial-interglacial CO₂ variations, *Global Biogeochem. Cycles*, 16, 10.1029/2001GB001446, 2002. [19](#)
- Gnanadesikan, A., Slater, R. D., Gruber, N., and Sarmiento, J. L.: Oceanic vertical exchange and new production: a comparison between models and observations, *Deep-Sea Res. II*, 49, 363–401, 2002. [5](#)
- Gosink, T. A., Pearson, J. G., and Kelley, J. J.: Gas movement through sea ice, *Nature*, 263, 41–42, 1976. [14](#)
- Heinrich, H.: Origin and consequences of cyclic ice rafting in the northeast Atlantic ocean during the past 130,000 years, *Quat. Res.*, 29, 142–152, 1988. [14](#), [15](#)
- Hodell, D. A., Venz, K. A., Charles, C. D., and Ninnemann, U. S.: Pleistocene vertical carbon isotope and carbonate gradients in the South Atlantic sector of the Southern Ocean, *Geochemistry, Geophysics, Geosystems*, 4, 1004, doi:10.1029/2002GC000367, 2003. [7](#)
- Hönisch, B. and Hemming, N. G.: Surface ocean pH response to variations in pCO₂ through two full glacial cycles, *Earth and Planetary Science Letters*, 236, 305–314, 2005. [18](#), [42](#)
- Howard, W. R. and Prell, W. L.: Late Quaternary CaCO₃ production and preservation in the Southern Ocean: Implications for oceanic and atmospheric carbon cycling, *Paleoceanography*, 9, 453–482, 1994. [16](#)
- Indermühle, A., Stocker, T. F., Joos, F., Fischer, H., Smith, H. J., Wahlen, M., Deck, B., Mastroianni, D., Tschumi, J., Blunier, T., Meyer, R., and Stauffer, B.: Holocene carbon-cycle dynamics based on CO₂ trapped in ice at Taylor dome, Antarctica, *Nature*, 398, 121–126, 1999. [18](#)
- Joos, F., Gerber, S., Prentice, I. C., Otto-Bliesner, B. L., and Valdes, P. J.: Transient simulations of Holocene atmospheric carbon dioxide and terrestrial carbon since the Last Glacial Maximum, *Global Biogeochemical Cycles*, 18, GB2002, doi:10.1029/2003GB002156, 2004. [4](#), [18](#)
- Jouzel, J., Lorius, C., Petit, J. R., Genthon, C., Barkov, N. I., Kotlyakov, V. M., and Petrov, V. M.: Vostok ice core: a continuous isotope temperature record over the last climate cycle (160 000 years), *Nature*, 329, 403–408, 1987. [2](#)
- Jouzel, J., Vimeux, F., Caillon, N., Delaygue, G., Hoffmann, G., Masson-Delmotte, V., and Parrenin, F.: Magnitude of isotopes/temperature scaling for interpretation of central Antarctic

- ice cores, *J. Geophys. Res.*, 108, 4361, doi:10.1029/2002JD002677, 2003. [7](#)
- Kawamura, K., Nakazawa, T., Aoki, S., Sugawara, S., Fujii, Y., and Watanabe, O.: Atmospheric CO₂ variations over the last three glacial-interglacial climatic cycles deduced from the Dome Fuji deep ice core, Antarctica using a wet extraction technique, *Tellus*, 55B, 126–137, 2003. [2](#)
- Knorr, G. and Lohmann, G.: Southern Ocean origin for the resumption of Atlantic thermohaline circulation during deglaciation, *Nature*, 424, 532–536, 2003. [3](#), [7](#)
- Kohfeld, K. E., Quere, C. L., Harrison, S., and Anderson, R. F.: Role of marine biology in glacial-interglacial CO₂ cycles, *Science*, 308, 74–78, 2005. [4](#)
- Köhler, P. and Fischer, H.: Simulating changes in the terrestrial biosphere during the last glacial/interglacial transition, *Global and Planetary Change*, 43, 33–55, doi:10.1016/j.gloplacha.2004.02.005, 2004. [5](#), [8](#), [9](#), [17](#)
- Köhler, P., Fischer, H., Munhoven, G., and Zeebe, R. E.: Quantitative interpretation of atmospheric carbon records over the last glacial termination, *Global Biogeochem. Cycles*, 19, GB4020, doi:10.1029/2004GB002345, 2005. [3](#), [4](#), [5](#), [6](#), [8](#), [18](#)
- Lisiecki, L. E. and Raymo, M. E.: A Pliocene-Pleistocene stack of 57 globally distributed benthic δ¹⁸O records, *Paleoceanography*, 20, PA1003, doi:10.1029/2004PA001071, 2005. [7](#), [9](#), [30](#)
- Martin, J. H.: Glacial-interglacial CO₂ change: the iron hypothesis, *Paleoceanography*, 5, 1–13, 1990. [3](#), [8](#)
- McManus, J. F., Oppo, D. W., and Cullen, J. L.: A 0.5-million-year record of millennial-scale climate variability in the North Atlantic, *Science*, 283, 971–975, 1999. [6](#), [7](#), [14](#), [30](#)
- McManus, J. F., Francois, R., Gheradi, J.-M., Keigwin, L. D., and Brown-Leger, S.: Collapse and rapid resumption of Atlantic meridional circulation linked to deglacial climate changes, *Nature*, 428, 834–837, 2004. [7](#)
- Meissner, K. J., Schmittner, A., Weaver, A. J., and Adkins, J. F.: Ventilation of the North Atlantic Ocean during the Last Glacial Maximum: a comparison between simulated and observed radiocarbon ages, *Paleoceanography*, 18, 1023, doi:10.1029/2002PA000762, 2003. [7](#), [8](#)
- Monnin, E., Indermühle, A., Dällenbach, A., Flückiger, J., Stauffer, B., Stocker, T. F., Raynaud, D., and Barnola, J.-M.: Atmospheric CO₂ concentrations over the last glacial termination, *Science*, 291, 112–114, 2001. [2](#)
- Morales-Maqueada, M. A. and Rahmstorf, S.: Did Antarctic sea-ice expansion cause glacial CO₂ decline?, *Geophys. Res. Lett.*, 29, doi:10.1029/2001GRL013240, 2001. [14](#)
- Munhoven, G.: Glacial-interglacial changes of continental weathering: estimates of the related

- CO₂ and HCO₃⁻ flux variations and their uncertainties, *Global and Planetary Change*, 33, 155–176, 2002. [4](#), [9](#)
- Paillard, D. and Parrenin, F.: The Antarctic ice sheet and the triggering of deglaciations, *Earth and Planetary Science Letters*, 227, 263–271, 2004. [19](#), [20](#)
- 5 Petit, J. R., Jouzel, J., Raynaud, D., Barkov, N. I., Barnola, J.-M., Basile, I., Bender, M., Chappellaz, J., Davis, M., Delaygue, G., Delmotte, M., Kotlyakov, V. M., Legrand, M., Lipenkov, V. Y., Lorius, C., Pépin, L., Ritz, C., Saltzman, E., and Stievenard, M.: Climate and atmospheric history of the past 420,000 years from the Vostok ice core, Antarctica, *Nature*, 399, 429–436, 1999. [2](#), [3](#), [10](#), [30](#), [33](#), [38](#), [39](#), [40](#)
- 10 Ridgwell, A. J.: Implications of the glacial CO₂ iron hypothesis for Quaternary climate change, *Geochemistry, Geophysics, Geosystems*, 4, 1076, doi:10.1029/2003GC000563, 2003. [3](#), [8](#)
- Ridgwell, A. J., Watson, A. J., Maslin, M. A., and Kaplan, J. O.: Implications of coral reef buildup for the late Quaternary carbon cycle, *Paleoceanography*, 18, 1083, doi:10.1029/2003PA000893, 2003. [18](#)
- 15 Röthlisberger, R., Mulvaney, R., Wolff, E. W., Hutterli, M. A., Bigler, M., Sommer, S., and Jouzel, J.: Dust and sea salt variability in central East Antarctica (Dome C) over the last 45 kyrs and its implications for southern high-latitude climate, *Geophys. Res. Lett.*, 29, 1963, doi:10.1029/GL015186, 2002. [2](#), [16](#)
- Ruddiman, W. F.: The anthropogenic greenhouse era began thousands of years ago, *Climatic Change*, 61, 261–293, 2003. [18](#)
- 20 Sachs, J. P. and Anderson, R. F.: Increased productivity in the subantarctic ocean during Heinrich events, *Nature*, 434, 1118–1121, 2005. [6](#), [14](#)
- Sarnthein, M., Pflaumann, U., and Weinelt, M.: Past extent of sea ice in the northern North Atlantic inferred from foraminiferal paleotemperature estimates, *Paleoceanography*, 18, 1047, doi:10.1029/2002PA000771, 2003. [7](#)
- 25 Schwander, J., Jouzel, J., Hammer, C. U., Petit, J.-R., Udisti, R., and Wolff, E.: A tentative chronology for the EPICA Dome Concordia ice core, *Geophys. Res. Lett.*, 28, 4243–4246, 2001. [13](#)
- Semiletov, I., Makshtas, A., and Akasofu, S.-I.: Atmospheric CO₂ balance: the role of Arctic sea ice, *Geophys. Res. Lett.*, 31, L05121, doi:10.1029/2003GL017996, 2004. [14](#)
- 30 Shackleton, N.: The 100 000-year ice-age cycle identified and found to lag temperature, carbon dioxide, and orbital eccentricity, *Science*, 289, 1897–1902, 2000. [30](#), [33](#), [38](#), [39](#), [40](#)
- Shackleton, N. J., Berger, A., and Peltier, W. P.: An alternative astronomical calibration of the

25

- lower Pleistocene timescale based on OPD site 677, *Trans. Royal Soc. Edinburgh: Earth Sciences*, 81, 251–261, 1990. [6](#), [30](#)
- Siddall, M., Rohling, E. J., Almogi-Labin, A., Hemleben, C., Meischner, D., Schmelzer, I., and Smeed, D. A.: Sea-level fluctuations during the last glacial cycle, *Nature*, 423, 853–858, 5 2003. [6](#), [14](#)
- Siegenthaler, U., Stocker, T. F., Monnin, E., Lüthi, D., Schwander, J., Stauffer, B., Raynaud, D., Barnola, J.-M., Fischer, H., Masson-Delmotte, V., and Jouzel, J.: Stable carbon cycle-climate relationship during the late Pleistocene, *Science*, 310, 1313–1317, doi:10.1126/science.1120130, 2005. [2](#), [3](#), [10](#), [20](#), [30](#), [33](#), [38](#), [39](#), [40](#)
- 10 Sigman, D. M. and Boyle, E. A.: Glacial/interglacial variations in atmospheric carbon dioxide, *Nature*, 407, 859–869, 2000. [3](#)
- Smith, H. J., Fischer, H., Wahlen, M., Mastroianni, D., and Deck, B.: Dual modes of the carbon cycle since the Last Glacial Maximum, *Nature*, 400, 248–250, 1999. [4](#)
- Stephens, B. B. and Keeling, R. F.: The influence of Antarctic sea ice on glacial-interglacial 15 CO₂ variations, *Nature*, 404, 171–174, 2000. [3](#), [13](#), [37](#)
- Toggweiler, J. R.: Variation of atmospheric CO₂ by ventilation of the ocean's deepest water, *Paleoceanography*, 14, 571–588, 1999. [3](#)
- Vecsei, A. and Berger, W. H.: Increase of atmospheric CO₂ during deglaciation: constraints on the coral reef hypothesis from patterns of deposition, *Global Biogeochem. Cycles*, 18, GB 1035, doi:10.1029/2003GB002147, 2004. [10](#)
- 20 Vimeux, F., Cuffey, K. M., and Jouzel, J.: New insights into Southern Hemisphere temperature changes from Vostok ice cores using deuterium excess correction, *Earth and Planetary Science Lett.*, 203, 829–843, 2002. [10](#)
- Visser, K., Thunell, R., and Stott, L.: Magnitude and timing of temperature change in the Indo-Pacific warm pool during deglaciation, *Nature*, 421, 152–155, 2003. [6](#)
- 25 Wang, Y., Mysak, L. A., and Roulet, N. T.: Holocene climate and carbon cycle dynamics: experiments with the green McGill Paleoclimate Model, *Global Biogeochemical Cycles*, 19, GB3022, doi:10.1029/2005GB002484, 2005. [18](#)
- Watson, A. J. and Garabato, A. C. N.: The role of Southern Ocean mixing and upwelling in 30 glacial-interglacial atmospheric CO₂ change, *Tellus B*, in press, 2006. [7](#)
- Wolff, E. W., Chappellaz, J. A., Fischer, H., Krull, C., Miller, H., Stocker, T., and Watson, A. J.: The EPICA challenge to the Earth System Modeling Community, *EOS*, 85, 363, 2004. [3](#)
- Wolff, E. W., Kull, C., Chappellaz, J., Fischer, H., Miller, H., Stocker, T. F., Watson, A. J.,

26

- Flower, B., Joos, F., Köhler, P., Matsumoto, K., Monnin, E., Mudelsee, M., Paillard, D., and Shackleton, N.: Modeling past atmospheric CO₂: results of a challenge, EOS, 86(38), 341, 345, 2005. 19, 20
- Wolff, E. W., Fischer, H., Fundel, F., Ruth, U., Twarloh, B., Littot, G. C., Mulvaney, R., Röthlisberger, R., de Angelis, M., Boutron, C. F., Hansson, M., Jonsell, U., Hutterli, M., Lambert, F., Kaufmann, P., Stauffer, B., Stocker, T. F., Steffensen, J. P., Bigler, M., Siggaard-Andersen, M. L., Udisti, R., Becagli, S., Castellano, E., Severi, M., Wagenbach, D., Barbante, C., Gabrielli, P., and Gaspari, V.: Southern Ocean sea ice, DMS production and iron flux over the last eight glacial cycles, Nature, in press, 2006. 16
- Wright, A. K. and Flower, B. P.: Surface and deep ocean circulation in the subpolar North Atlantic during the mid-Pleistocene revolution, Paleoceanography, 17, 1068, doi:10.1029/2002PA000782, 2002. 6, 14, 15, 30
- Zeebe, R. E. and Westbroek, P.: A simple model for the CaCO₃ saturation state of the ocean: the Strangelove, the Neritan, and the Cretan Ocean, Geochemistry, Geophysics, Geosystems, 4, 1104, doi:10.1029/2003GC000538, 2003. 4

27

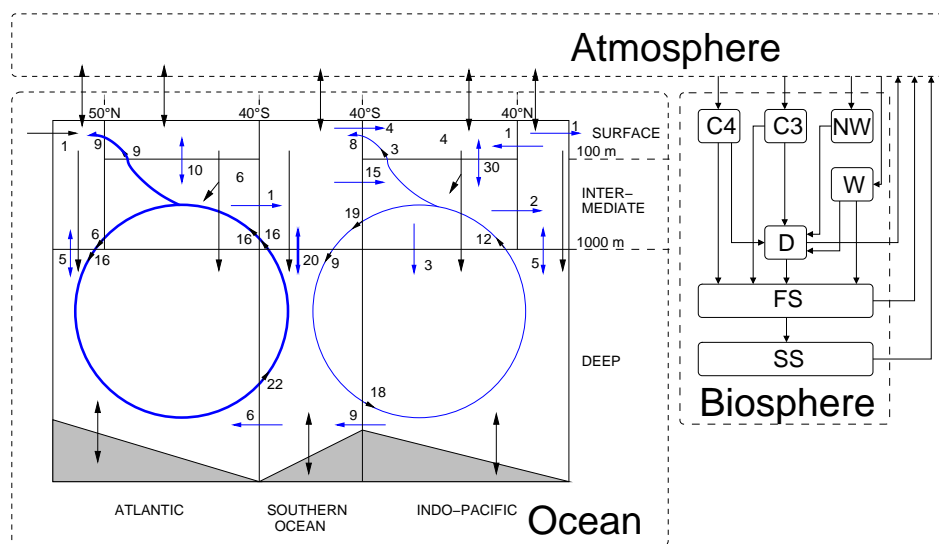


Fig. 1. Geometry of the Box model of the Isotopic Carbon cYCLE (BICYCLE). Carbon fluxes between different reservoirs are shown in black. Biosphere compartments: C₄: C₄ ground vegetation; C₃: C₃ ground vegetation; NW: non-woody parts of trees; W: woody parts of trees; D: detritus; FS: fast decomposing soil; SS: slow decomposing soil. Ocean: Recent fluxes of ocean circulation (in Sv=10⁶ m³ s⁻¹) are shown in blue based on the World Ocean Circulation Experiment WOCE (Ganachaud and Wunsch, 2000). Bold arrows indicate those fluxes in ocean circulation (NADW formation and subsequent fluxes; Southern Ocean vertical mixing) which are changed over time.

28

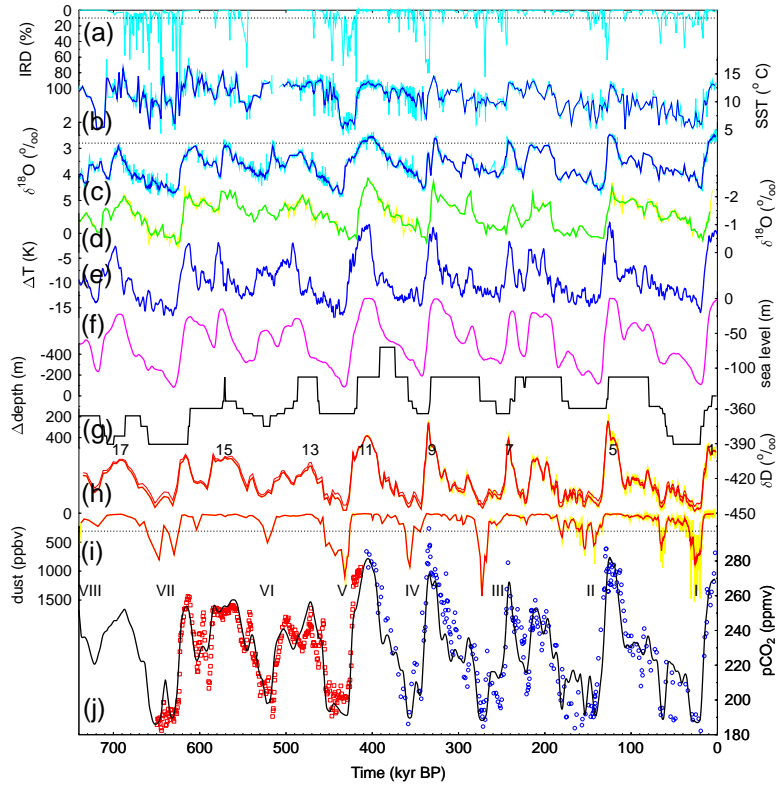


Fig. 2.

29

Fig. 2. Paleo-climatic records which were used to force the BICYCLE model (a–i) and measured and simulated $p\text{CO}_2$ (j). Ice rafted debris IRD (a), SST reconstructions (b), and benthic $\delta^{18}\text{O}$ in foraminifers (c) from the sediment core drilled at the site ODP980 (55°29' N, 14°42' W) (McManus et al., 1999; Flower et al., 2000; Wright and Flower, 2002). (d): Planktic $\delta^{18}\text{O}$ of ODP677 (1°12' N, 83°44' W) (Shackleton et al., 1990). Reconstructed (e) temperature changes over land in the northern hemisphere (40–80° N) and (f) sea level changes, both after Bintanja et al. (2005), based on a benthic $\delta^{18}\text{O}$ stack from 57 sediment cores (Lisiecki and Raymo, 2005). (g): Changes in the depth of the Pacific lysocline (Farrell and Prell, 1989). Original (thin) and sea level corrected (bold) deuterium δD (h) and atmospheric dust contents (i) as measured in the EPICA Dome C ice core (EPICA community members, 2004). (j): Measured $p\text{CO}_2$ from Vostok (blue circles) (Petit et al., 1999) plotted on the orbitally tuned age scale (Shackleton, 2000), from EPICA Dome C (red squares) (Siegenthaler et al., 2005), and simulated $p\text{CO}_2$ (5 kyr running mean) of our standard scenario (line). Data prone to high frequency fluctuations (b, c, d, h, i) were used as 3 kyr running means. Numbers in panel (h) label interglacial MIS, the Latin numbers in panel (j) count the last eight terminations. Horizontal lines in (a, b and i) mark certain thresholds.

30

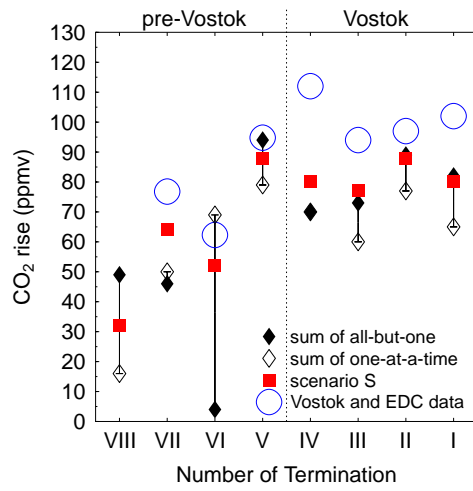


Fig. 3. Estimating the rise in $p\text{CO}_2$ between minima and maxima crossing Terminations I to VIII by various methods. Vostok and EPICA Dome C $p\text{CO}_2$ data are compared to our standard scenario S, and to the summation of the two different single process identifications methods used in Fig. 6 (one-process-at-a-time vs. all-but-one-processes).

31

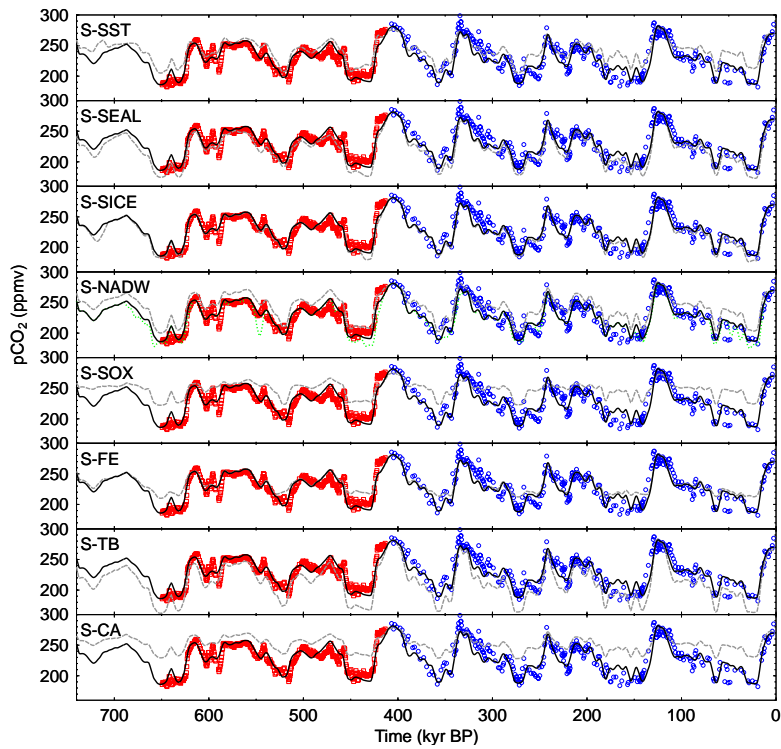


Fig. 4.

32

Fig. 4. Analysis of single processes on atmospheric $p\text{CO}_2$ in comparison to the Vostok $p\text{CO}_2$ record (Petit et al., 1999) (blue circles) which was plotted on the orbitally tuned age scale (Shackleton, 2000), and the EPICA Dome C $p\text{CO}_2$ (red squares) record (Siegenthaler et al., 2005). All processes (standard simulation S, bold black) and all but one process at a time (dash grey) were forced externally. Processes depict changes in SST (S-SST), sea level (S-SEAL), sea ice (S-SICE), NADW formation (S-NADW), Southern Ocean vertical mixing (S-SOX), iron fertilisation in the Southern Ocean (S-FE), carbon storage in terrestrial biosphere (S-TB), sediment/ocean exchange fluxes of DIC and alkalinity (S-CA). Additionally, a scenario with all processes at work and a complete shut-down of NADW formation during all Heinrich events as indicated by IRD in the North Atlantic was simulated (short-dash green in subfigure S-NADW). As the inclusion of exchange fluxes between sediment and ocean is converting our modelled carbon cycle to an open system in which total carbon and alkalinity are not conserved anymore a direct comparison between individual simulations becomes difficult due to variations in the overall budgets. All simulation results are shown as 5 kyr running mean.

33

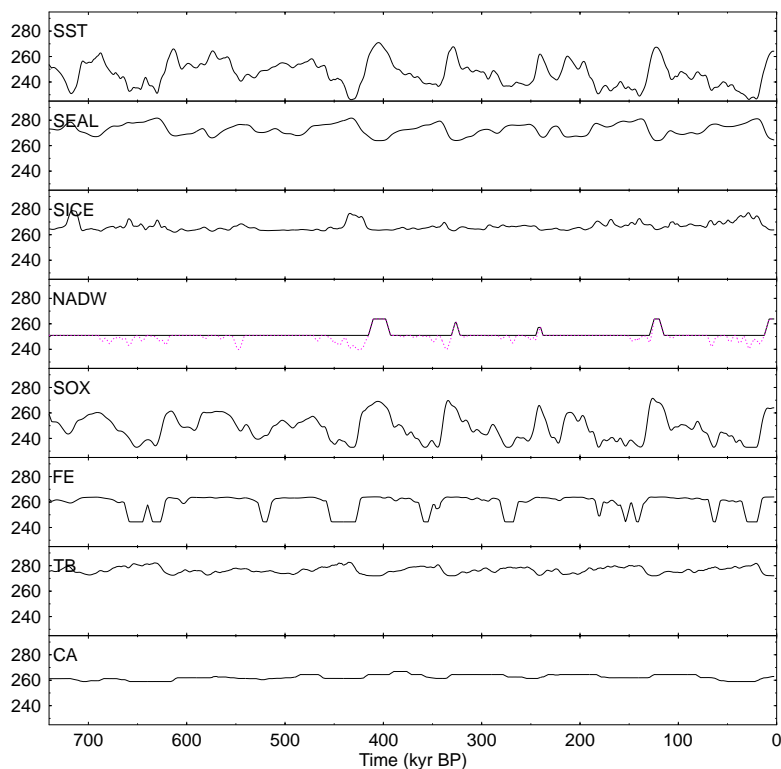


Fig. 5.

34

Fig. 5. Analysis of the effect of single processes on atmospheric $p\text{CO}_2$. One process at a time was forced externally while all other forcings were held constant at preindustrial level. Considered processes depict changes in SST (SST), sea level (SEAL), sea ice (SICE), NADW formation (NADW), Southern Ocean vertical mixing (SOX), iron fertilisation in Southern Ocean (FE), carbon storage in terrestrial biosphere (TB), sediment/ocean exchange fluxes of DIC and alkalinity (CA). Additionally, a scenario with variable NADW formation including its shut-down during Heinrich events is shown (dashed in subfigure NADW). In TB the effect of CO_2 fertilisation is underestimated leading to a glacial/interglacial variation in terrestrial carbon storage of only 130 PgC in comparison to more than 1000 PgC in our standard scenario. In CA only the effect of changes in the lysocline are depicted, as all other responses of the sediment/ocean fluxes depend on the other processes which were not changed over time here. All simulation results are shown as 5 kyr running mean.

35

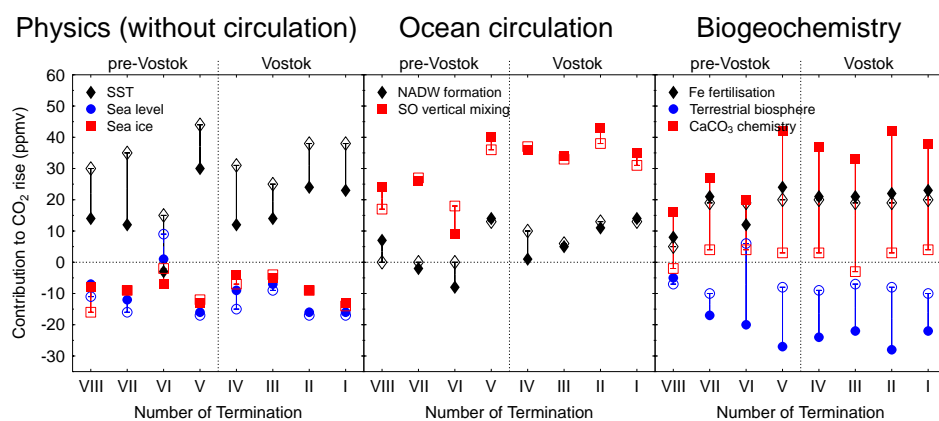


Fig. 6. Impact of different processes on glacial/interglacial changes in $p\text{CO}_2$ during the last eight terminations. We estimate single process contributions by either the time-dependent forcing of one process only (open symbols), or by calculating the differences between simulation S and the simulation which excludes the time-dependent forcing of the process in question (filled symbols). Shown here are the contributions to the $p\text{CO}_2$ rise between minima and maxima crossing Terminations I to VIII. Full time-dependent results underlying our analysis here are found in Figs. 4 and 5. The processes are sub-grouped into physics (excluding ocean circulation), ocean circulation, and biogeochemistry and include changes in SST, sea level, gas-exchange through sea ice, NADW formation, Southern Ocean vertical mixing, iron (Fe) fertilisation of marine biology in the Southern Ocean, terrestrial biosphere, and DIC and alkalinity fluxes between deep ocean and sediment (CaCO_3 chemistry). Differences between filled and open symbols highlight the high non-linearity of the system. CaCO_3 chemistry analysed as single effect contains only the changes in the depth of the lysocline, but changing DIC and alkalinity budgets of the deep ocean through other processes in combined scenarios will lead to fluxes one order of magnitude higher. The terrestrial carbon storage in the one-at-a-time approach underestimates the effect of CO_2 fertilisation leading to a glacial/interglacial variation in terrestrial carbon storage of only 130 PgC in comparison to more than 1000 PgC in our standard scenario.

36

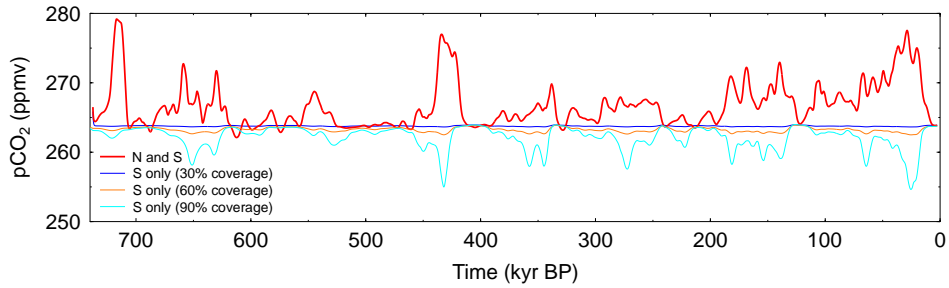


Fig. 7. Northern and southern contributions to the impact of sea ice cover on atmospheric $p\text{CO}_2$ in a single processes analysis. In the reference run (N and S) nearly no contribution comes from the Southern Ocean sea ice, which covers during LGM 30% of the Southern Ocean surface box area. Increasing this Southern Ocean sea ice areal cover up to 90% coverage shows opposing trends (reduced $p\text{CO}_2$ during glacial times) from the northern contribution (increased $p\text{CO}_2$ during glacial times). This Southern Ocean behaviour is in line with previous investigations (Stephens and Keeling, 2000). All simulation results are shown as 5 kyr running mean.

37

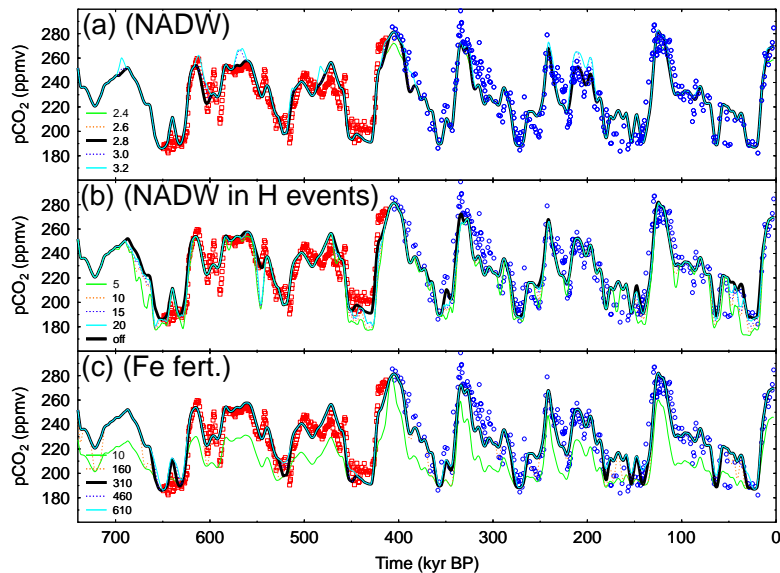


Fig. 8. Variation of fixed threshold values used during simulations. Simulation results were shown as 5 kyr running mean. Bold depicts always the standard simulation S using the standard values, blue circles the Vostok $p\text{CO}_2$ data (Petit et al., 1999) on the orbitally tuned age scale (Shackleton, 2000), red squares the EPICA Dome C $p\text{CO}_2$ data (Siegenthaler et al., 2005). **(a):** Varying the threshold $\delta^{18}\text{O}_{\text{NADW}}$ in ODP980 which indicates changes in the strength in the NADW formation ($\delta^{18}\text{O}_{\text{NADW}}=2.4, 2.6, 2.8, 3.0, 3.2\%$). **(b):** Varying the threshold in IRD as the indicator for Heinrich events measured in ODP980 ($\text{IRD}_H=5, 10, 15, 20\%$). Note, that in our standard scenario the NADW formation during identified Heinrich events is not shut-down. **(c):** Varying the threshold in the atmospheric dust content as measured in EPICA Dome C which is a proxy for the onset of iron fertilisation in the Southern Ocean ($\text{dust}_{\text{Fe}}=10, 160, 310, 460, 610$ ppbv).

38

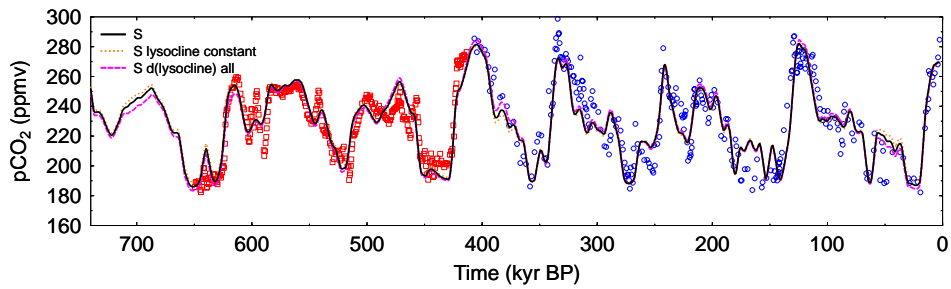


Fig. 9. Variations in lysocline dynamics. Beside the standard simulation S, in which only the lysocline in the Pacific Ocean is varied two alternative scenarios were tested. First, the lysocline in all ocean basins is varied, second the lysocline in all ocean basin is kept constant. Data from the Vostok $p\text{CO}_2$ record (Petit et al., 1999) (blue circles) which was plotted on the orbitally tuned age scale (Shackleton, 2000), and the EPICA Dome C $p\text{CO}_2$ (red squares) record (Siegenthaler et al., 2005) are also shown. All simulation results are shown as 5 kyr running mean.

39

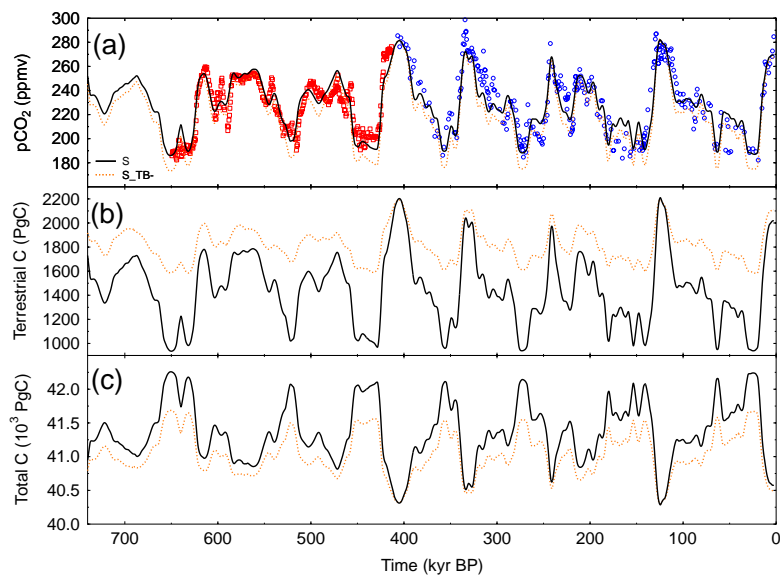


Fig. 10. Additionally to the standard simulation S an alternative pathway of terrestrial biosphere regrowth was considered (S_TB-). **(a):** Atmospheric $p\text{CO}_2$. Data from the Vostok $p\text{CO}_2$ record (Petit et al., 1999) (blue circles) which was plotted on the orbitally tuned age scale (Shackleton, 2000), and the EPICA Dome C $p\text{CO}_2$ (red squares) record (Siegenthaler et al., 2005). **(b):** Terrestrial carbon storage. **(c):** Total carbon storage in the atmosphere/ocean/biosphere system. Glacial/interglacial rise in terrestrial carbon during Termination I was 500 and 1100 PgC in scenario S_TB- and S, respectively, covering the range deduced from other modelling and data based studies. All simulation results are shown as 5 kyr running mean.

40

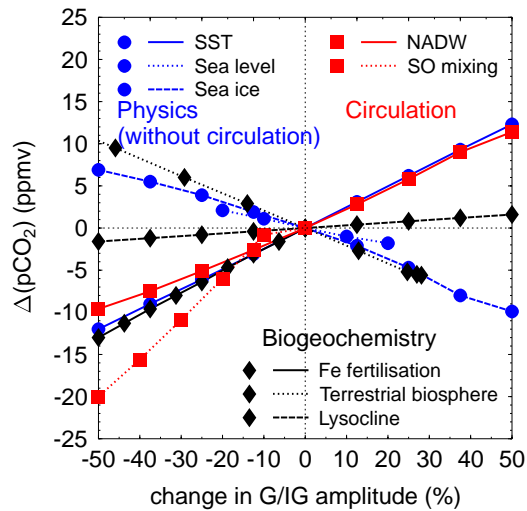


Fig. 11. Sensitivity analysis of the impact of the glacial/interglacial amplitudes of the individual processes on the rise in atmospheric $p\text{CO}_2$ during the last glacial/interglacial transition covering Termination I (30–0 kyr). Differences from the rise in $p\text{CO}_2$ as function of amplitudinal changes in individual processes during combined scenarios (all processes included) from the reference runs are shown. Processes depict changes in SST, sea level, gas-exchange rate through sea ice, NADW formation, Southern Ocean vertical mixing, iron (Fe) fertilisation in the Southern Ocean, carbon storage in terrestrial biosphere, the depth of the Pacific lysocline. Note, that the exchange fluxes of DIC and alkalinity between deep ocean and sediment can not be changed in their amplitudes. Glacial/interglacial amplitude of sea level change was varied only $\pm 20\%$ due to high reliability of known sea level change. The glacial/interglacial amplitudes of iron (Fe) fertilisation, and Southern Ocean vertical mixing (Southern Ocean mixing) could only be reduced as they were operating on their possible upper limit.

41

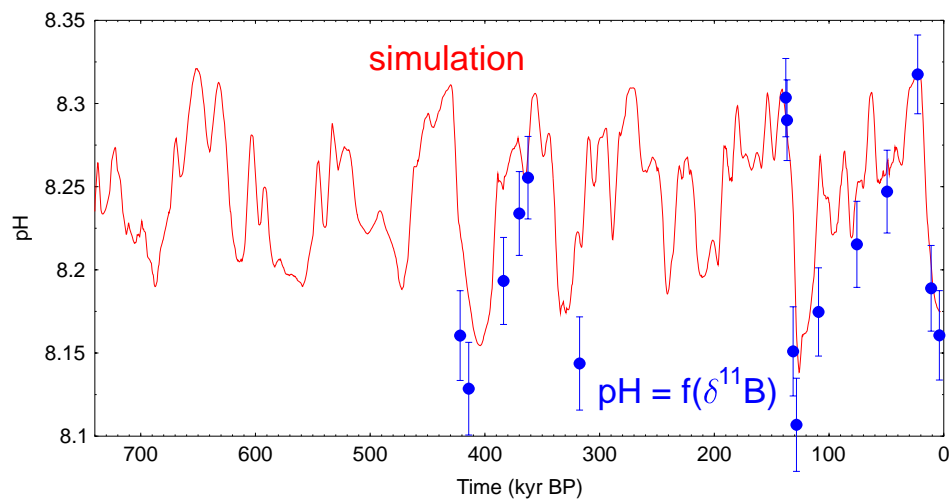


Fig. 12. Comparison of simulated pH in the equatorial Atlantic surface box with pH reconstruction based on boron isotopes $\delta^{11}\text{B}$ measured in planktic foraminifers (Hönisch and Hemming, 2005). All simulation results are shown as 5 kyr running mean.

42